ORIGINAL ARTICLE

Open Access

Impact of coating and microstructure on wear resistance of tool steels for wood cutting: a novel approach to quantification and analysis of wear-related damages

Vanella Mbakop Nanshie[1] , Ali Aidibe[1], Majid Heidari[2] and Mohammad Jahazi[1*]

Abstract

Squaring, a wood transformation process, is an operation which consists of introducing the logs into a squaring machine which then uses sharp tools to cut the wood into pieces with high surface quality. Tool steels used in this process experience significant wear, damaging the wood surface and hence leading to substantial scrape rate. This study investigates the wear resistance of three tool steels specifically designed for wood cutting applications: modified AISI A8, modified steels with 0% and 1% tungsten, and powder metallurgy prepared W360 steel. Furthermore, the influence of a PVD coating on the wear resistance of the three alloys was investigated. ASTM G65 abrasive wear tests were conducted using the dry sand/rubber wheel abrasion test. A methodology using a non-contact 3D measurement system and specialized software was developed, allowing for a thorough quantitative assessment of the wear of these steels. The results revealed that the coated A8mod + 1%W steel exhibits the best resistance among the coated steels. Despite the excellent intrinsic resistance of W360 steel, the coating did not provide a significant improvement for this steel, showing only a 10% reduction in wear. Microstructural analysis revealed that the predominant wear mechanisms were abrasion and impact. The relative performance of each steel was quantified and is reported. Field trials conducted under actual cutting conditions, indicate the superiority of W360 steel in terms of resilience to wear and impacts compared to other tested alloys, while confirming the effectiveness of surface treatments in mitigating material wear. However, A8 steel modified with 1% tungsten exhibits increased wear under coating.

Keywords Wear resistance, Wear mechanisms, Wear test, Influence of microstructure on wear, PVD coating, Quantification of wear, Tool edge, Wood cutting, Non-contact 3D measurement system, Scanning and digitization procedure

*Correspondence:
Mohammad Jahazi
mohammad.jahazi@etsmtl.ca
[1] Mechanical Engineering Department, École de Technologie Supérieure (ÉTS), Montreal, QC, Canada
[2] DK-Spec, Lévis, QC, Canada

Introduction

Wood machining, despite its relatively lower hardness compared to other materials such as metals and plastics, holds a prominent position in the global industrial landscape [1]. It is widely used in various industries, including the furniture industry, construction, flooring, and musical instrument manufacturing. However, wood machining faces significant challenges, particularly the premature wear of tools, leading to increased production costs and interruptions and can compromise the quality

Mbakop Nanshie *et al. Journal of Wood Science*   (2024) 70:20

Page 2 of 15

of the final product as well. Wood, due to its intrinsic nature, possesses unique characteristics that can accelerate tool wear; hence necessitating meticulous attention during its machining [2, 3]. Its relative hardness, abrasiveness, and sensitivity to moisture, combined with potential knots and inclusions, place additional stresses on tools [4, 5]. The tool–machine interaction is also a key factor in tool wear. Friction, variations in properties of the workpiece, and cutting conditions can all contribute to accelerated wear [6, 7]. The major issues encountered in the wood industry include premature wear, primarily caused by the ductility of the cutting tool, steel, and material detachment from impacts by foreign objects such as nails, beads, stones, etc. [8, 9]. The wear damage typically arises from a combination of mechanisms, including abrasion, adhesion, fatigue, and corrosion, all influenced by a variety of factors [10–14]. It has been reported that abrasion wear is the predominant damage mode in secondary wood cutting processes [15].

The great majority of materials used in the wood cutting industry are composed of tool steels. They are characterized by their moderate carbon content (0.5% wt) and a substantial amount of alloying elements such as Cr, Mo, and W which form carbides with a large spectrum of composition, size, morphology and distribution that determine the resistance to abrasive wear [16]. Although tool design [17], positioning in the equipment [18], and type of wood [19] influence tool durability, tool material has the biggest impact on wear life of wood cutting tools [18, 20].

Given the critical implications of tool wear, its accurate assessment becomes of paramount importance. The traditional wear evaluation methods often employed in the industry consist of either simple visual inspection, which is very subjective with a large margin of error, or the 2D approach, which consists in cutting the worn tool in few places and measuring the wear damage. The latter method has several shortcomings including the fact that it is a destructive method, requires tedious manual processing, and does not account for the entire length of the worn edge due to the non-uniform nature of wear. Confronted with these challenges, the quest for a wear quantification method that seamlessly blends accuracy with practicality for the wood industry becomes indispensable. In recent years, with the advent of modern non-contact 3D imaging technology, innovative methods have been proposed to quantify wear. Bagga et al. [21] has developed a system for directly measuring tool wear by employing image processing techniques. Jeon et al. [22] employed a technique for measuring cutting tool wear by using knife-edge interferometry (KEI). Lee et al. has developed a simplified method based on the direct analysis of the three-dimensional scanning data of the worn specimen without requiring a separate reference scan [23]. These methods, although promising, require specific expertise and complex implementation, which underscores the need for a fast, accurate, and reliable method which can be readily applicable in the industry.

Based on the above review of the available literature, the primary objective of this study is to assess the influence of alloy composition, coating, and microstructure on wear damage in wood cutting tool steels. Additionally, the study aims to identify the most effective steel in terms of wear resistance and contribute to a better understanding of wear phenomena in squaring knives. We also introduce an innovative method to quantify the wear of wood-cutting tools. This approach aims to provide an optimal solution for measuring wear without compromising the tool's integrity, while meeting the precision and speed requirements essential in the industrial context.

Principles of the new methodology

The current method for quantifying wear relies on comparing high-resolution data from the same surface before and after wear, by scanning new samples for measuring total volume, and then subsequently scanning samples after use to determine wear parameters, and finally subtracting the volume of worn samples from new ones to establish the volume of wear. Although other evaluation/measurement techniques can be used as well, only the Keyence microscope was used in this study.

Previous wear assessments often relied on point-by-point measurements and direct measurements of tool geometry, based on cross-sectional cuts of worn knives. This often led to not considering the entire worn edge, potentially resulting in underestimation or overestimation of wear due to the potential heterogeneity of wear along the edge.

The wear quantification methodology used in this study is robust, allowing for a detailed analysis of tool steels. Scans before and after wear provide a clear and accurate representation of knife conditions at different stages of use, enabling a detailed comparison of wear over time. Semi-automated, it reduces human error and potentially enhances measurement reproducibility. Crucially, this method encompasses the entire edge, providing a more holistic representation of wear. Additional information such as lost volume and wear profile can also be extracted, offering a thorough understanding of wear dynamics and severity. Furthermore, its non-destructive nature is particularly advantageous, preserving samples for future analyses.

Mbakop Nanshie *et al. Journal of Wood Science* (2024) 70:20

Page 3 of 15

Materials and method

The three tool steels studied include modified AISI A8 with 0% tungsten (identified as A0W), modified AISI A8 with 1% tungsten (identified as A1W), and AISI W360, a powder metallurgy tool steel. Table 1 presents the chemical compositions of these steels obtained by using a SPECTROMAXx (LMX10), an optical emission spectrometer. The coating was applied using the physical vapor deposition (PVD) method. The coating composition consists of AlTiN for the first layer and AlTiCrN for the second layer, with a total thickness of 3.9 μm, applied using a PL1011 apparatus manufactured by PLATIT [24].

Two series of wear damage evaluation experiments were conducted: wear tests according to the ASTM G65 standard and field trials. For each series, specific samples were manufactured. The knife edges and micro-bevels sharpened at the company (knife manufacturer). The field trials involved the use of squaring knives on six samples, three uncoated and three coated ones, while the ASTM G65 tests were conducted with rectangular samples measuring 25 × 76mm and a thickness of 12.7 mm, with 3 samples for each type of steel and condition [25].

Table 2 summarizes the experimental plan, and Fig. 1 illustrates sample dimensions used in the present study.

The wear test machine uses the standard ASTM G65. The test uses rectangular specimens of 25 × 76 mm with a thickness of 12.7 mm. Here, procedure B in the ASTM G65 standard test was adopted with a test duration of 10 min. This procedure is recommended by the ASTM G65 standard for the more abrasion-resistant materials or annealed low-carbon steel [25]. The volume loss is calculated using the formula provided by Eq. (1), recommended by the standard ASTM G65:

$$\text{Volume loss}\left(\text{mm}^3\right) = \frac{\text{Mass loss }(\text{mg})}{\text{Density of material }(\text{g/cm}^3)}. \tag{1}$$

After each test, a visual observation of anomalies was initially conducted, followed by microscopic and microstructural analysis. For microstructural analysis, standard

**Table 1** Chemical composition of tool steels

AISI/SAE	C	Cr	Mo	W	V	Si	Mn	Ni	Cu
A0W[a]	0.516	7.76	1.27	0.0768	0.338	0.832	0.326	0.368	0.121
A1W[b]	0.538	7.93	1.17	1.05	0.077	0.786	0.375	0.144	0.0385
W360	0.513	4.43	3.08	0.0296	0.565	0.226	0.221	0.0778	0.0451

[a] A0W = A8mod + 0%W = modified A8 with 0% tungsten

[b] A1W = A8mod + 1%W = modified A8 with 1% tungsten

Table 2 Experimental plan

Test	Steel type	Condition	Number of samples	Total number of samples	Sample types	Test duration
Wear test	A0W, A1W and W360	Coated and uncoated	3 per types of steel per types of condition	18	Rectangular specimens	10 min
Field test	A0W, A1W and W360	Coated and uncoated	3 per types of steel per types of condition	18	Squaring knives	124 h
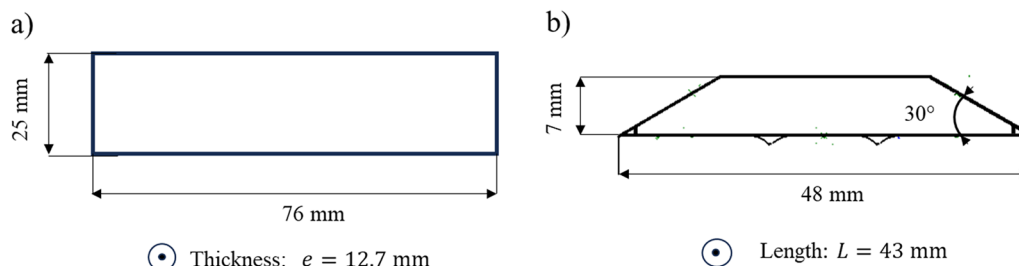
Fig. 1 Sample dimensions for **a** wear test and **b** field test

Mbakop Nanshie *et al. Journal of Wood Science*   (2024) 70:20

Page 4 of 15

metallographic sample preparation was followed, consisting of abrasive cutting of the hot mounting, then mirror polishing with 1 micron diamond paste, and finally chemical etching with 3% Nital to reveal the steel's microstructure.
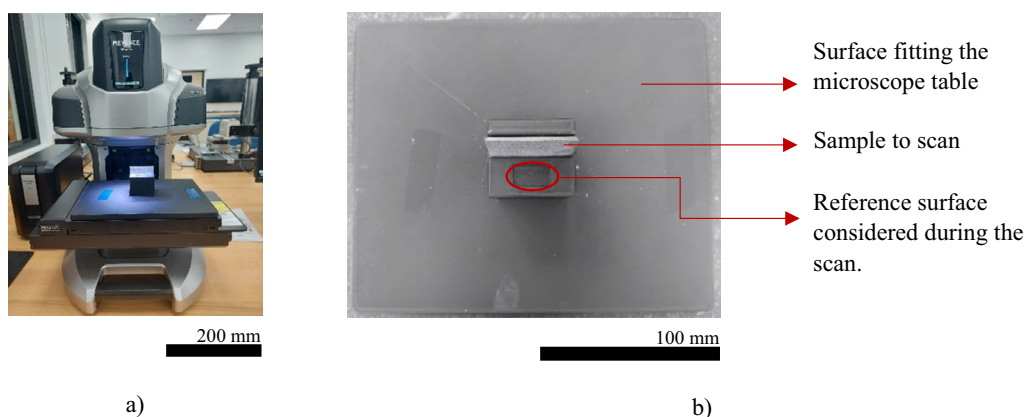
Following this preparation, a microstructural examination using a Hiatchi TM3000 scanning electron microscope (SEM) was performed. Additionally, chemical analysis was conducted using optical emission spectrometry, complemented by energy-dispersive X-ray spectroscopy (EDX) analysis in the SEM to ensure the reliability of the results. The hardness of the various steels was assessed using a durometer, and HRC hardness measurements using10 kgf and 150 kgf loads, providing indications of their relative strengths. Finally, the JmatPro software was employed to determine the phases present in the material, offering a comprehensive view of its composition and intrinsic properties.

The quantification of wear involves several steps. Initially, a scan of the knives was performed before the wear test. This scan produced a digital representation of the new knives in their pristine state. The resultant data act as a visual and geometric reference, making it possible to compare the knife's condition before and after usage in order to subsequently assess the extent of wear on the cutting edge. After their usage in wood-cutting operations, the knives were scanned again. Scanning the worn knives provides a digital depiction of the cutting edge after exposure to the cutting action. This scan visualizes geometric changes and identifies wear signs such as deformations or cutting-edge fractures.
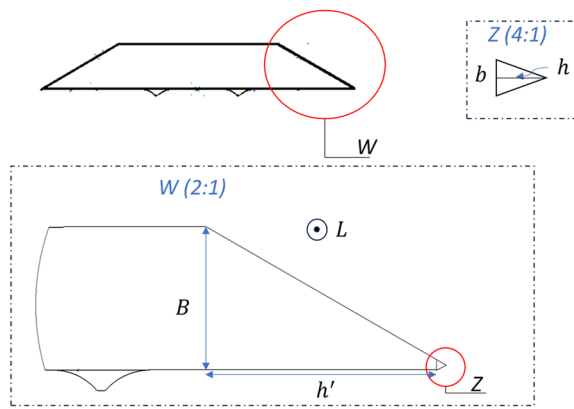
The proposed approach utilizes a high-resolution microscope (Fig. 2a), with a display resolution (height measurement) of 0.1 µm to conduct pre- and post-wear scans of knives. The repeatability of these scans is documented as 0.5 µm at high resolution and 1 µm at low resolution [26]. The measurement accuracy at low magnification, where a wide field of view is employed, is within ± 5 µm. However, at high magnification, the measurement accuracy improves, achieving a precision of ± 2 µm [26]. In this study, brand-new knives were meticulously positioned on a specially designed holder, then scanned following a stringent procedure. The sample holder (Fig. 2.b), was custom 3D-printed to cater to the unique needs of the experiment. This holder was specifically designed to securely position the specimens, enabling effortless manipulation, which is important from the perspective of industrial implementation as well as that of detailed microscopic observation. Similarly, worn-out knives were subjected to the same identical scanning protocol. The obtained scan data, both from the new and worn knives, were analyzed utilizing the microscope's integrated software and exported to Python computational platforms to estimate the volume lost by wear.

The edge of a new cutting tool is the sharp area that directly interacts with the wood being machined. When viewed in cross-section, the configuration of the edge reveals a distinct morphology, consisting of two sections. The first is the trapezoidal base that serves as a support for the cutting edge. The second is the triangular tip, representing the effective cutting edge of the tool. The volume of this edge ($VE_{Theoretical}$) can be estimated by calculating the volume of the trapezoid and adding it to the volume of the triangular tip (Fig. 3). In this context, b is the base of the triangle and the shorter base of the trapezoid, B is the longer base of the trapezoid, h is the height of the triangle, and h' is the height of the trapezoid. This leads us to the formula defined by Eq. (2):

a)   b)

Fig. 2 **a** Keyence microscope, **b** sample holder

Surface fitting the microscope table

Sample to scan

Reference surface considered during the scan.

200 mm

100 mm

with $h = 3$ mm, $b = 2$ mm *et* $h' = 11.5$ mm

Fig. 3 Presentation of the cutting edge. "W (2:1)" and "Z (4:1)" are magnification rates

Volume of edge

$$= \mathrm{VE}_{\mathrm{theoretical}} = \left[\left(\frac{b \times h}{2} \right) + \left(\frac{(B + b) \times h'}{2} \right) \right] \times L, \quad (2)$$

with $h = 3\ mm$, $b = 2\ mm$ and $h^{'} = 11.5\ mm$.

Digitization of samples for field test

The scanning of samples allows for a precise digital representation of their condition. As mentioned above, in order to accurately and reliably quantify the wear performance of different tool steels, it is of paramount importance to have an accurate estimation of the wear damage over the *entire* length of the knife, and not a very limited zone. The resulting data provide a visual and geometric reference for comparing sample conditions before and after use, hence making it possible to assess the extent of wear on the cutting edges. Figure 4 illustrates a set of pre-wear and post-wear scans of a sample.

Using this method for the evaluation of wood cutting tools, it is possible to select and study a specific area of the worn surface, eliminating the need for smooth initial surfaces. It also allows focusing on areas that do not exhibit severe wear without compromising the overall integrity of the tool. The defined zone will be referred to as the volume edge recession (VER). It is determined by calculating the difference between the initial volume of the knives before wear ($\mathrm{VE}_{\mathrm{beforewear}}$) and the final volume after a specified period of use ($\mathrm{VE}_{\mathrm{afterwear}}$).

Estimation of lost volume for field test

To further quantify wear, one must determine the volume lost by wear. It is determined by calculating the difference between the initial volume of the knives before wear and the final volume after a specified period of use. The method employs knife scans exported as 3D stl files which enable use in Python. This technique facilitates the determination of wear volume.

Illustration

To illustrate our analysis, we are examining a sample subjected to a specific duration of work. The initial step, involving digitizing the sample before and after wear, allows us to obtain the digitized images along with their respective volumes in each case. The outcomes of this procedure are presented in Fig. 4.

Following digitization, the obtained result for wear-induced volume loss is as follows: wear volume loss $= 21.14\ \mathrm{mm}^3$. Simultaneously, an assessment of wear parameters according to ISO 3685 standard [27] can be conducted. Extracted measurements are depicted in Fig. 5.

Results and discussion

Analysis of tool steel characteristics

Scanning electron microscopy of the tools revealed a microstructure composed of a martensitic matrix scattered with primary carbides. The EDX analysis of A0W steel revealed a high concentration of precipitates primarily composed of Cr, Mn, V, and Mo. The A1W steel has a similar composition to the A0W with the difference of the 1% tungsten. Tungsten is added to enhance the formation of carbides as well as to increase solid solution hardening [28]. In contrast to the two other steels, the W360 steel shows a more pronounced presence of molybdenum and vanadium carbides and finer grain size due to its preparation route, powder metallurgy.

The phase diagram of the three steels reveals a complex variety of phases coexisting at different compositions and temperatures. Generally, liquid, ferrite, austenite, and M(C,N) phases are present in all three steels. The M23C6 phase is predominant in each steel, suggesting its key role in determining the mechanical properties. A0W steel is distinguished by the exclusive presence of the M7C3 phase, absent in the other two steels, which could specifically influence its properties [29]. Both A1W and W360 steels contain the M6C phase, which could contribute to distinctive properties [29] compared to A0W steel. Table 3 compiles results from microstructural analysis, presenting an overview of the key microstructural characteristics of the studied materials. It includes details on transition temperatures, and other relevant information,

	Digitized Knife		Obtained Volume (mm³)
Before Wear			2595.52
After Wear			2574.38

Fig. 4 Digitized result

aiming to provide a quick and efficient reference for key data.

The hardness of the three alloys were measured using the HRC scale, better adapted for high hardness materials. HRC hardness measurements using 10 kgf and 150 kgf loads were conducted. Here, the combination of these two loads allows for a precise evaluation of the material hardness. The initial pre-load of 10 kgf ensures that the indenter is properly in contact with the material surface, while the total load of 150 kgf performs the actual measurement of the material's hardness [30].

Table 4 summarizes hardness values obtained for the three steels. The results indicate variability in measurements. The standard deviations indicate the errors associated with these measurements, reflecting potential variability in the sample structure. Such variations are crucial considering the direct impact of hardness on material wear resistance, where higher hardness values are generally correlated with better resistance [16]. Consequently, the steel with the highest Rockwell hardness could be expected to exhibit enhanced performance in terms of wear resistance. However, a comprehensive assessment must consider other factors as well.

Evaluation of abrasive wear

Following ASTM G65 standard testing procedure, wear tests were conducted for the three steels and the obtained results are depicted in Table 5. The abrasive wear progression was tracked based on cycle count, where 1000 cycles corresponded to a 5-min test duration. In the present study, a total test duration of 10 min was considered, and sample weights were measured before and after the test with a high precision balance ($\pm$ 1 mg).
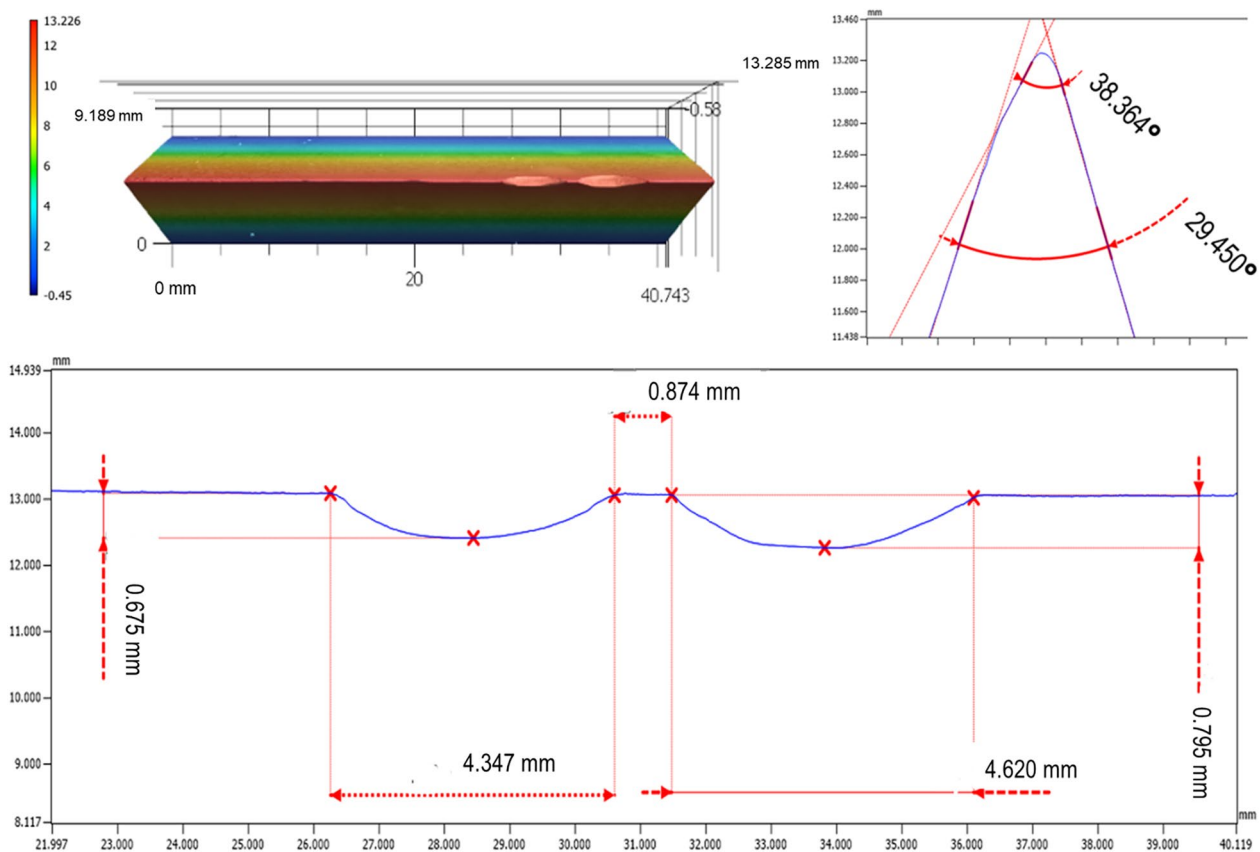
Mbakop Nanshie *et al. Journal of Wood Science*   (2024) 70:20

Page 7 of 15

Fig. 5 Profile measurement

Table 3 Summary of the results obtained from the microstructural analysis

Samples	A0W	A1W	W360
Microstructure	Fine martensitic	Martensitic	Fine martensitic
Lath size	5.5 ± 0.5 μm	13.2 ± 3.4 μm	4.1 ± 1.0 μm
Carbide size	1.1 ± 0.4 μm	0.9 ± 0.2 μm	0.8 ± 0.24 μm
M(C,N) carbide	V, Nb	Nb	V
M(C,N) Diss. Temp	1130 ℃	1205 ℃	1147 ℃
M7C3 carbide	Cr	–	–
M7C3 Diss. Temp	1060 ℃	–	–
M6C carbide	–	W	Mo
M6C Diss. Temp	–	981 ℃	1032 ℃
M23C6 carbide	Cr, Fe	Cr, Fe	Cr, Fe
M23C6 Diss. Temp	1010 ℃	1044 ℃	916 ℃

Table 4 Rockwell hardness results

Steel	A0W	A1W	W360
Rockwell hardness (HRC)	55.91 ± 1.14	54.33 ± 1.05	54.29 ± 1.07

The quantification methodology we developed, which will be detailed in section Materials and method, was applied to assess the volume loss of each sample, as detailed in Table 6. A slight difference (10% maximum) is observed between the results obtained using the ASTM G65 standard and those obtained by the application of the new method, which is attributable to the conversion factor (material density) used in the ASTM G65 standard. Unlike this standard, our method directly measures the volume by assessing the wear depth on the sample. It is important to note that the density used in the ASTM G65 standard is that of the raw material with a nominal composition and under ideal conditions (i.e., absence of any porosity, inclusion, etc.) which could be different from the actual density.

The wear rate was calculated by the ratio of the mass loss to the sliding distance, as also reported in other works [29] and the results are reported in Fig. 6.

The obtained results reveal that the application of the PVD coating has resulted in significant improvement in wear resistance for the A1W and A0W steels, 49% and 39%, respectively. In contrast, for W360 steel, the coating appears less effective, offering a minimal 10%

Table 5 Results of wear test

| Sample	Number of specimens	Mass loss (mg)	Density (g/cm^3)	Volume loss (mm^3)
Coated A1W	3	339.67 ± 26.63	7.8	43.46 ± 3.41
Uncoated A1W	3	675 ± 11.53		86.57 ± 1.47
Coated A0W	3	380.67 ± 32.13	7.7	49.48 ± 4.17
Uncoated A0W	3	636.33 ± 6.81		82.60 ± 0.88
Coated W360 steel	3	381 ± 12.50	7.6	50.13 ± 1.64
Uncoated W360 steel	3	436 ± 16.37		57.37 ± 2.15

Table 6 Volume loss using the developed method for quantification of wear

Steel type	Number of specimens (per case)	Volume loss Coated steel (mm^3)	Volume loss Uncoated steel (mm^3)
A1W	3	40.67 ± 4.11	87.72 ± 4.97
A0W	3	57.89 ± 8.23	90.67 ± 1.94
W360	3	46.65 ± 3.57	59.30 ± 8.77

Fig. 6 Wear rate of steels

reduction in wear. It is also interesting to note that, without coating, W360 steel performs the best. It is also worth mentioning that abrasion wear tests prove to be crucial informative tools for evaluating the potential of coatings under specific wood cutting conditions [31]. The above results are in agreement with those reported by Krzysztof Nadolny and al. [32] who reported that CrCN/CrN-based PVD coating appears to significantly improve the performance of industrial planer knives by reducing wear, increasing durability and maintaining superior cut quality.

Additional tests were conducted on the three steels to further quantify the influence of coating on their wear resistance. To this end, an additional 30-min wear test was conducted for one sample per case. The objective was to observe the coating's behavior for different steel grades and the evolution of wear over the number of wheel cycles. The results are illustrated in Fig. 7.

Examining the wear evolution for A0W steel (Fig. 7), a consistent mass loss is observed for both coated and uncoated samples. However, careful observation of the first 2000 cycles for the coated steel is crucial. Indeed, it reveals a lower mass loss during this initial phase, before adopting a linear trend from the 2000 cycles upward. A similar observation is noted for A1W steel. However, a distinctive feature is evident for the coated W360 steel during the first 2000 cycles compared to other steels. For both coated and uncoated steels, the mass loss trend is linear and consistent over the entire 6000 cycles of the wheel. The results suggest that, for A8 mod steels, the applied coating reduces wear propagation, thereby
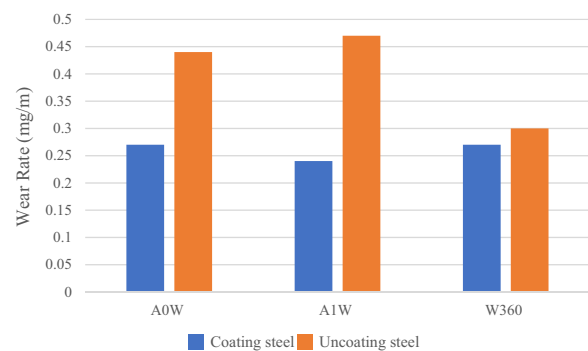
decreasing wear compared to W360. Although W360 exhibited good performance without coating, no notable difference is observed with the coated version, indicating an ineffectiveness of the coating on this steel grade.

Wear and damage mechanisms of tool steels for field test
Figure 8 is an illustrative example of the state of degradation of sample knives after 124 h of work. Visual observations revealed notable material detachments on certain coated knives, suggesting potential vulnerability of these samples. This implies that the coated A1W may have wear resistance limitations. Moreover, coated steels exhibit reduced wear compared to the uncoated ones. These findings indicate that coatings can enhance wear resistance and extend knife longevity under abrasive conditions. Furthermore, the results reveal that the uncoated A1W knives appear to present the best resistance to abrasive wear. Consequently, it may offer a balanced trade-off between shock resistance and wear durability, contingent upon specific application requirements.

Table 7 summarizes the wear mechanisms observed in each case, thus providing a better understanding of how these factors interact and influence the wear resistance of these materials.

In order to identify the microstructure related wear mechanisms, samples from the three steels were

Mbakop Nanshie *et al. Journal of Wood Science* (2024) 70:20

Page 9 of 15
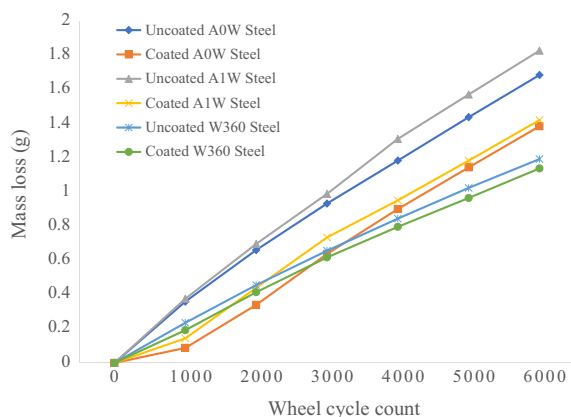
**Fig. 7** Progression of the lost mass for each steel

examined. A scanning electron microscopy (SEM) analysis is conducted to observe these mechanisms in detail. Figure 9 shows typical SEM micrographs for A1W steel and provides a detailed view of the effects of wear on the material surface of the steel.

The presence of craters (Fig. 9a and d) resulting from the wear process, is prominently visible, illustrating areas where material has been removed or eroded over time. These craters may vary in size and depth, providing insights into the intensity of wear experienced by the surface. Simultaneously, evident signs of plastic deformation (Fig. 9c and e) are observed in the region surrounding the craters. These plastic deformations attest to the stresses and forces the material has endured during the wear process, leading to permanent alterations in its

structure. Furthermore, scratches (Fig. 9b) resulting from abrasive wear are clearly identifiable on the material surface. These linear marks highlight the relative movement between the material and its wear environment, emphasizing the areas most subjected to abrasion during the process.

Figure 10 provides SEM images for the knives made of the A0W steel. The analysis showed the behavior of this steel is similar to the A1W case, though a significant number of cracks were observed near the chipped zones, indicating the lower toughness of this steel compared to the A1W one. Typical examples are shown in Fig. 10c, d where cracks are clearly visible around the chipped zones.

In contrast with the two other steels, knives made of W360 steel exhibits no evident degradation, aside from some edge recession (Fig. 11e). This is particularly noteworthy considering that all three steels were subjected to the same working conditions. Microstructural examples in Fig. 11 illustrate that fewer signs of deterioration are present, suggesting that W360 steel demonstrates superior impact resistance compared to the other two steels. Clear signs of impact wear (Fig. 11a) are visible in the microstructure, suggesting that the steel has been subjected to impact stresses during its use. These impact marks result from the heterogeneous nature of wood, repeated impacts, or interaction with abrasive particles such as sand and gravel present on the wood chips [15]. Moreover, evident chipping (Fig. 11d) is observed along the edge of the W360 steel. These chips indicate areas where the material has detached, likely due to higher local stresses or stress concentration. The presence of
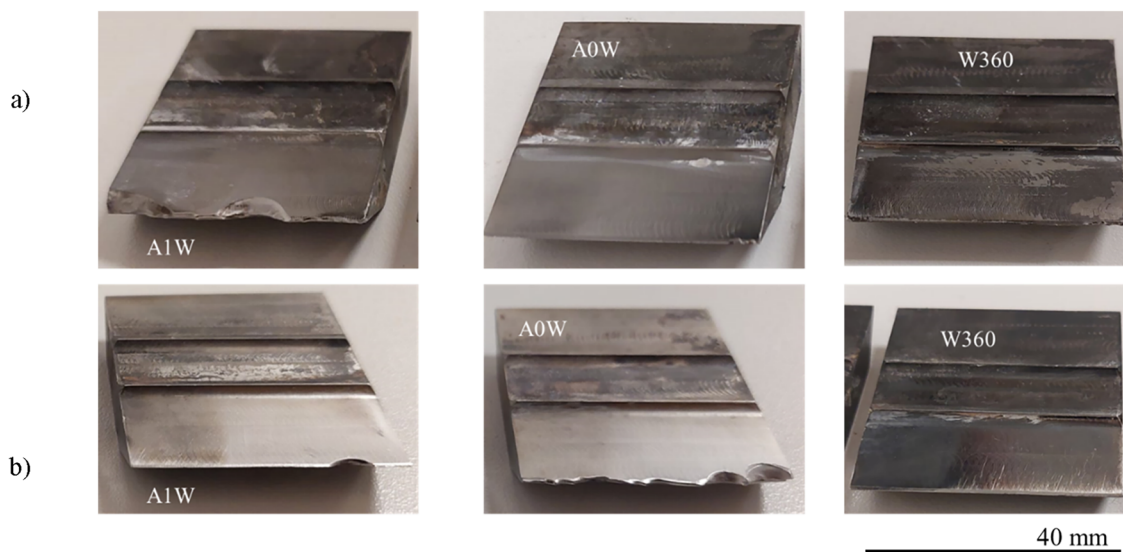

Fig. 8 Worn knives: **a** coated and **b** uncoated

Mbakop Nanshie *et al. Journal of Wood Science*   (2024) 70:20

Page 10 of 15

Table 7 Wear mechanisms observed in the three investigated steels

| Failure	Uncoated steels			Coated steels		
	A1W	A0W	W360	A1W	A0W	W360
Abrasive wear						
Reduction of edge sharpness	x[a]	x	x	x	x	x
Grooves	x	x	x	x	x	x
Edge degradation	x	x	x	x	x	x
Adhesive wear						
Craters		x		x		
Material tearing		x		x		
Impact wear						
Edge chipping	x	x	x	x	x	x
Microcracks		x		x		
Plastic deformation		x		x		

[a] x means that we find this type of wear on the steel
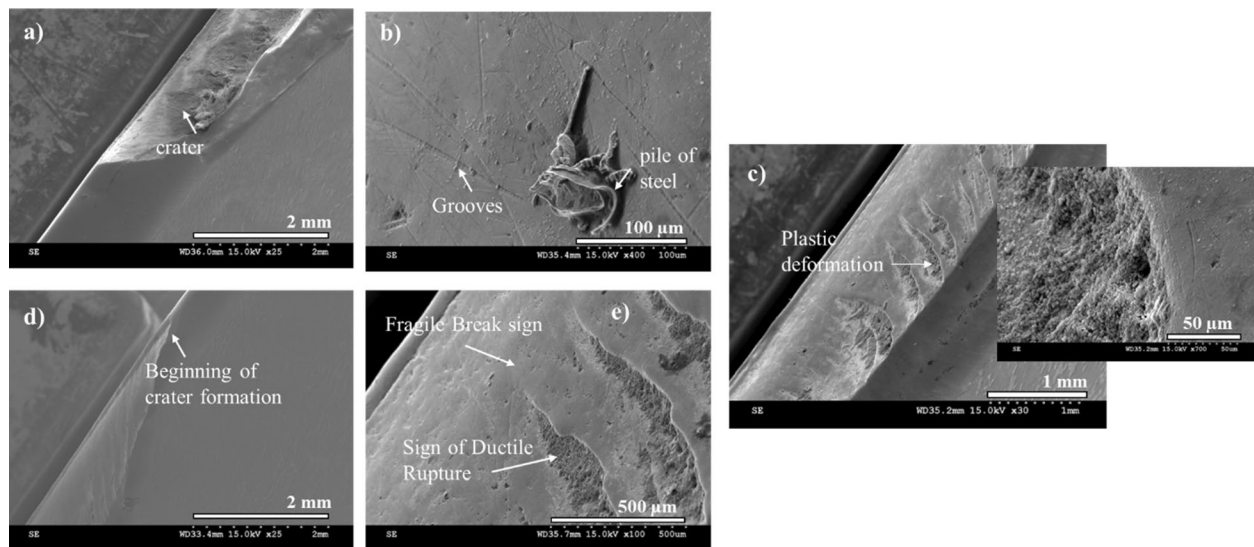

Fig. 9 Wear damage of A1W steel

these chips underscores the vulnerable zones on the surface, susceptible to significant mechanical stresses [33]. Additionally, discernible grooves (Fig. 11b) are present, resulting from abrasion wear. These grooves may be caused by continuous friction with abrasive particles or rough surfaces during the working process. The presence of these marks of abrasion wear highlights the material's interaction with external elements and underscores the need for increased resistance to abrasion to maintain the integrity of the steel surface [34].

Based on the above results it can be concluded that the W360 steel does not necessarily align with conventional trends observed in the literature [28] regarding

tool steel properties. It displays exceptional wear resistance, surpassing the other two steels in the experiment. It is interesting to note that, as reported by many authors [28, 35–37]) typically high-chromium tool steels are known for their superior abrasion resistance [38], those containing tungsten and tungsten carbide are known for their abrasive wear resistance [39], high-nickel, manganese, and silicon steels are reputed for their fatigue resistance [40], and high-tungsten and molybdenum steels are commonly used for erosion resistance [37]. However, the exceptional wear resistance of the W360 steel, despite its atypical chemical composition compared to the available literature, highlights the complex interactions between
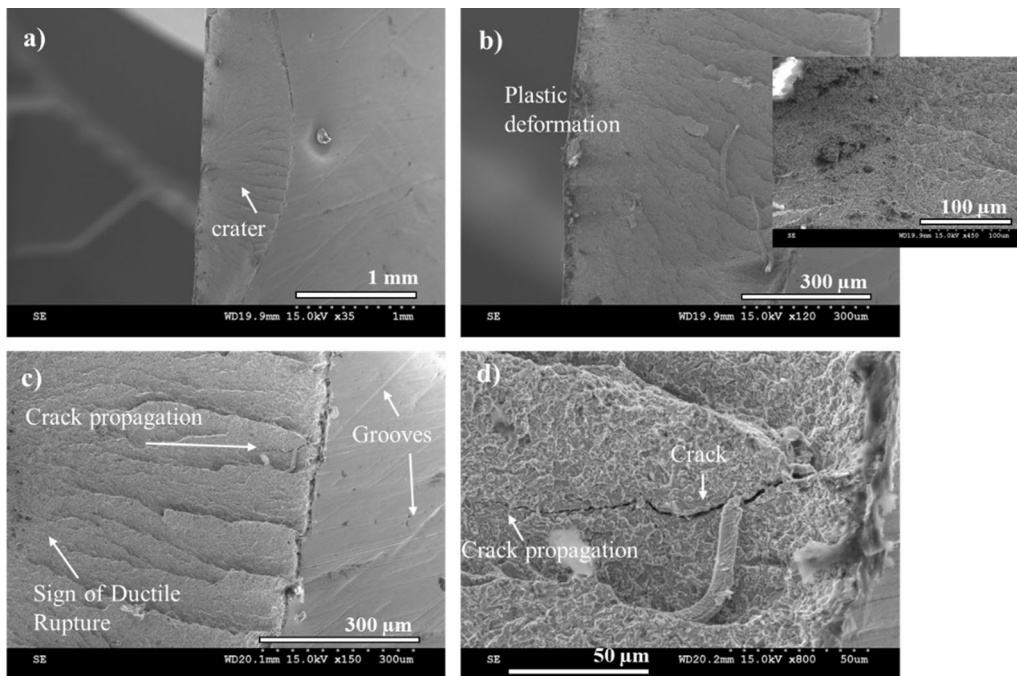
Fig. 10 Wear damage of A0W steel
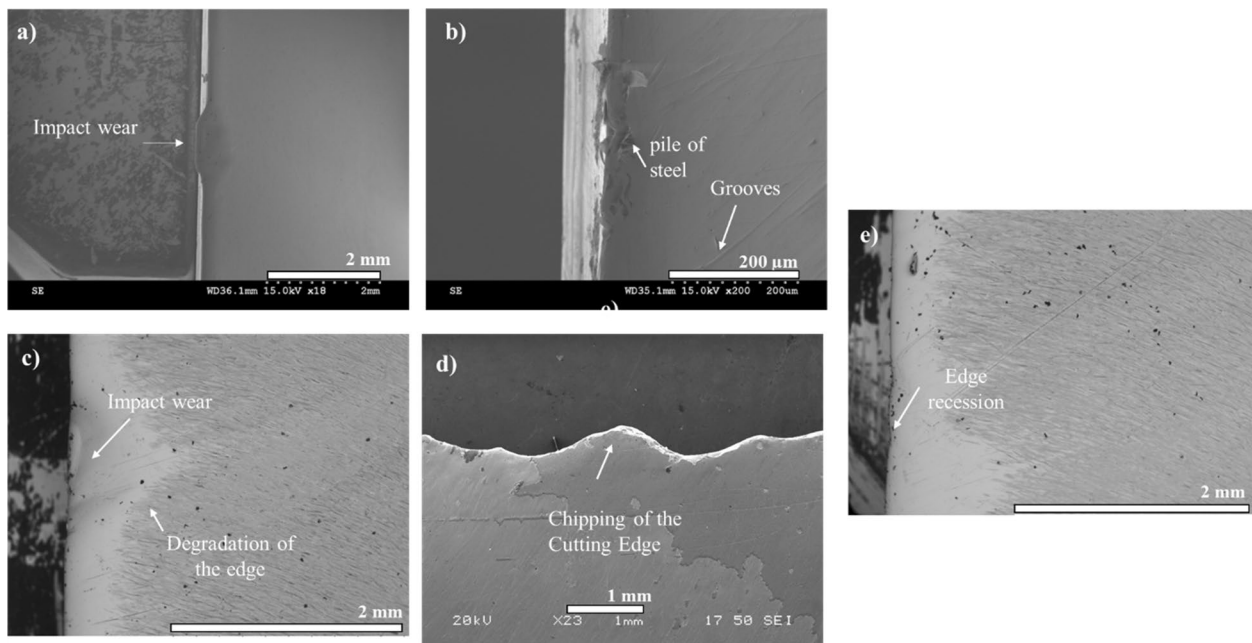
Fig. 11 Wear damage of W360 steel

alloy compositions and preparation (powder metallurgy here) that influence the operating wear mechanisms and overall wear resistance of tools used in the wood cutting industry. Furthermore, it is noteworthy that among the wear mechanisms observed for the three investigated steels, abrasive wear and impact wear appear to be the most predominant ones. These observations suggest that under the envisaged application conditions, these wear

mechanisms play a pivotal role in determining the durability and performance of the knives.

Wear volume loss

An assessment of knife wear was conducted, and the results obtained from the measurements of sample volume are summarized in Table 8. When comparing coated and uncoated steels, with reference to the VER coatings applied to the knives play a crucial role in reducing wear.

Focusing on coated steels, it is observed that W360 steel exhibits the lowest wear loss among them, highlighting superior resistance to wear for this specific composition. As for uncoated steels, A0W stands out by displaying the lowest wear loss. This observation suggests that even among uncoated steels, differences in composition have a significant influence on wear resistance. In summary, these results not only demonstrate the positive impact of coatings in reducing wear, but also highlight significant nuances among different types of steel, whether coated or uncoated.

ANOVA analysis to explore the relative contribution of alloy type and coating on wear resistance

In this section, we discuss the analysis of variance (ANOVA), a crucial statistical technique used to compare the means of multiple groups to identify any significant variance, thus offering an understanding of the interaction between the studied variables.

This study aims to evaluate the wear resistance of renderer knives by measuring volume loss after 124 h of work. The dependent variable is volume loss in mm^3. The

main objective is to determine whether there is a significant difference in volume loss between three different types of alloys (A0W steel, A1W and W360 steel) with two distinct coating factors (coated and uncoated). Thus, we have two factors of interest: the alloy type with three levels and the coating condition with two levels. These levels are quantitative and fixed.

For the experiment, two samples ($n=2$ replicates) of each combination of factors is used, resulting in a total of 12 samples. The order of verification of these samples is completely randomized to eliminate any potential bias. The significance level chosen for this analysis is 5%, indicating our threshold for determining whether the observed differences are statistically significant. The data are in Table 9.

Two-factor analysis of variance (two-factor ANOVA) will be used to analyze the data. This method will allow us to understand not only the effect of each factor individually (alloy type and coating factor) on volume loss, but also to determine whether a significant interaction exists between these two factors.

Definitions of assumptions

The assumptions can be defined as follows:

- Assumptions for the alloying factor:

  – Null hypothesis (H0): there is no significant difference in volume loss between different alloy types.
  – Alternative hypothesis (H1): there is a significant difference in volume loss between two or more types of alloy.

- Assumptions for the coating factor:

  – Null hypothesis (H0): there is no significant difference in volume loss between coating factors (coated and uncoated).
  – Alternative hypothesis (H1): there is a significant difference in volume loss between coating factors.

- Assumptions for the Interaction between alloy and coating:

Table 8 Volume loss of steels

	Steel	Number of specimens	Wear loss volume (mm^3)	VER[a] (mm^3)
Coated	A1W	3	44.54 ± 21.18	2.26 ± 1.72
	A0W	3	15.09 ± 1.71	2.24 ± 0.83
	W360	3	15.48 ± 2.96	1.68 ± 1.14
Uncoated	A1W	3	21.28 ± 6.77	3.49 ± 0.49
	A0W	3	34.99 ± 19.7	2.99 ± 1.4
	W360	3	18.66 ± 5.29	3.01 ± 1.69

[a] VER = volume edge recession = volume loss for a delimited zone

Table 9 Data table of volume loss for ANOVA

Sample	A0W steel		A1W steel		W360 steel	
	Coated	Uncoated	Coated	Uncoated	Coated	Uncoated
1	16.67	15.49	24.23	30.14	12.52	27.30
2	16.91	15.11	22.50	25.72	12.50	19.63

Table 10 Analysis of variance summary

Source	DL	Contribution	F-value	P-value
Alloy type	2	52.87%	15.17	0.005
Coating factor	1	16.82%	9.65	0.021
Alloy type * coating factor	2	19.86%	5.70	0.041
Error	6	10.45%		
Total	11	100.00%		

Table 11 Theoretical values of F [41]

Source	Alloy type	Coating factor	Alloy type * coating factor
$F_{theoretical}$	$F_{0.95,2,6} = 5.14$	$F_{0.95,1,6} = 5.99$	$F_{0.95,2,6} = 5.14$

– Null hypothesis (H0): there is no significant interaction between alloy type and coating factor on volume loss.
– Alternative hypothesis (H1): there is a significant interaction between alloy type and coating factor on volume loss.

Analysis of variance (ANOVA)

Analysis of variance in Table 9 gives the results compiled in Table 10.

In order to test the H0 null hypothesis for each factor, the use of the Fisher statistic is ideal. It allows us to compare the calculated value of F (F_{test}) with the theoretical value of F ($F_{theoretical}$). The latter is obtained from the Fisher table. The theoretical values corresponding to each source of variation are specified in Table 11.

Since in all cases we have $F_{test} > F_{theoretical}$, the null hypothesis is therefore rejected for both factors (alloy type and coating factor) and for the interaction (alloy type * coating factor). This indicates that the alloy and the coating factor (coated or uncoated) have a significant effect of 5% on the volume loss, and that the effect of one factor depends on the other factor. Figure 12 displays the residual plot for "Volume loss", demonstrating a uniform spread of points around zero, implying homogeneity of variances. Additionally, the distribution of residuals forms a relatively straight line, suggesting that the assumption of normality of residuals is likely satisfied.
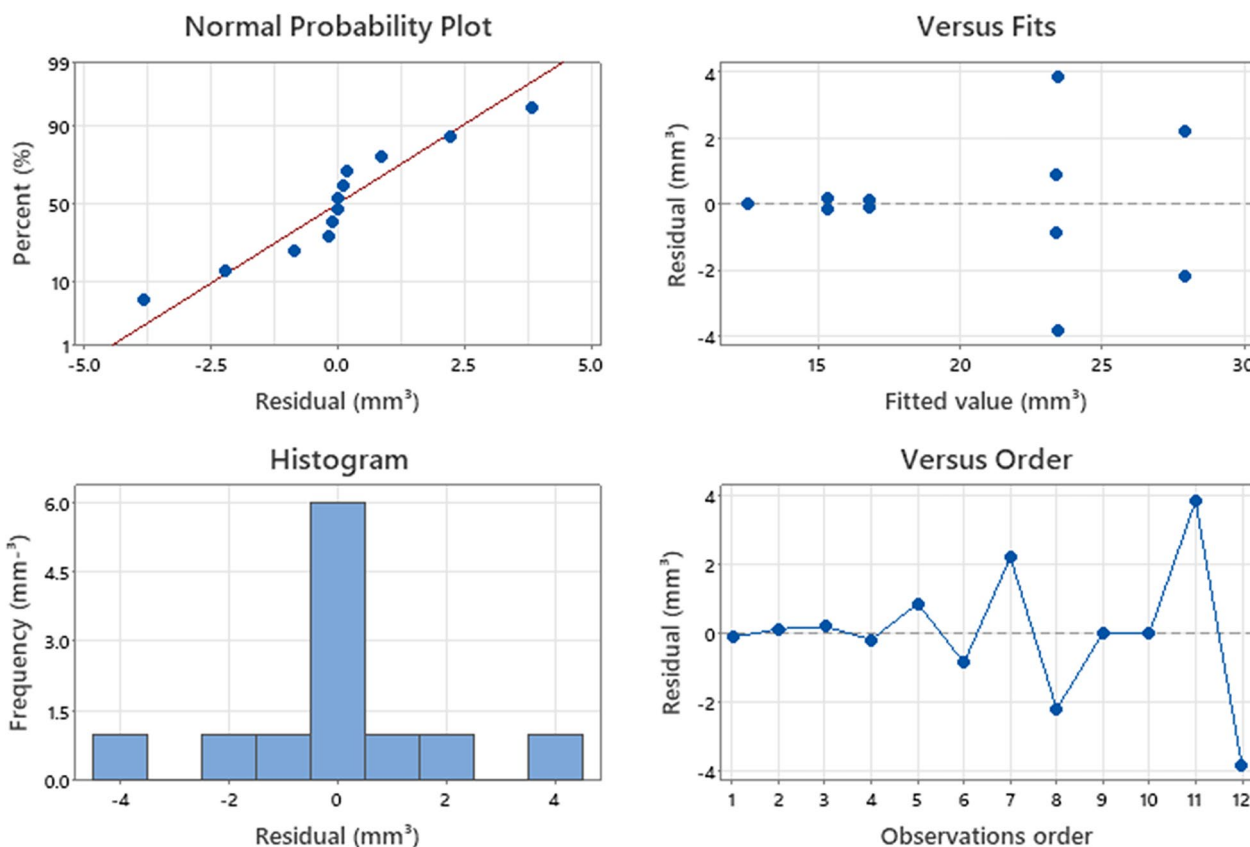
Fig. 12 Residual plots for volume loss (mm³)

Conclusion

- The wear resistance of steels depends not only on their chemical composition, but also on their microstructural characteristics, necessitating a holistic approach in material selection.
- W360 steel has demonstrated outstanding resistance to both wear and impacts, highlighting that chromium content alone is not the sole determinant of abrasion resistance. The presence of elements like molybdenum and vanadium, along with specific microstructural features, play a crucial role.
- The methodology, based on high-resolution microscopy and detailed software analysis, offers a level of precision and depth unmatched by traditional 2D methods.
- The study underscores the transformative impact of PVD coatings, demonstrating their ability to significantly enhance wear resistance, even for steels that are inherently sensitive.

The following recommendations suggest potential avenues for further exploration and enhancement of the current study, aiming for a more holistic understanding of tool wear mechanisms and assessment techniques:

- Linking observed damages to physical phenomena: investigating how the observed tool wear can be directly linked to specific physical wear mechanisms.
- Deep dive into coatings: while the article briefly touched upon the role of coatings in wear resistance, there's potential for a more comprehensive study on various coatings, their properties, and how they interact with different wood species.
- Comparative analysis of 3D methodology: a detailed comparative study could be undertaken to understand how the new 3D method stacks up against existing wear measurement techniques, pinpointing its advantages or possible shortcomings.
- Expanding beyond wood: although the primary focus of this study was on wood, could this methodology be applied to other materials? Exploring its potential applicability in other industries might provide broader insights.

Abbreviations

VER	Volume edge recession
A1W	Modified A8 with 1% tungsten
A0W	Modified A8 with 0% tungsten
SEM	Scanning electron microscopy
EDX	Energy-dispersive X-ray
ASTM	American Society for Testing and Materials
MATLAB	MATrix LABoratory
STL	Standard Triangle Language
% wt	Weight percentages
KEI	Knife-edge interferometry
PVD	Physical vapor deposition
ANOVA	Analysis of variance

Author contributions
V.M.N.: methodology, investigation, performed the experiments and analyzed, formal analysis, and writing—original draft preparation; A.A.: supervision, formal analysis, review, and editing; M.H.: formal analysis, review, and editing; M.J.: validation, writing—review and editing, supervision, project administration and funding acquisition. All authors have read and agreed to the final manuscript.

Availability of data and materials
No, as there are some industrial data.

Declarations

Competing interests
The authors certify the absence of any competing interests.

References
1. Triboulot P (2016) Le bois dans la construction: réflexions sur les évolutions probables et conséquences pour l'amont de la filière. Rev For Fr. https://doi.org/10.4267/2042/61861
2. Elloumi I, Hernández RE, Cáceres CB, Blais C (2021) Effects of temperature and moisture content of logs on size distribution of black spruce chips produced by a chipper-canter at two cutting widths. BioResources 16:6684–6705
3. Kuljich S, Hernández RE, Blais C (2017) Effects of cutterhead diameter and log infeed position on surface quality of black spruce cants produced by a chipper-canter. Wood Fiber Sci 49:235–248
4. Bendikiene R, Keturakis G (2017) The influence of technical characteristics of wood milling tools on its wear performance. J Wood Sci 63:606–614
5. Cristóvão L (2013) Machining properties of wood tool wear, cutting force and tensioning of blades. Dissertation, Luleå University of Technology, Luleå
6. Abdelali HB (2013) Caractérisation et modélisation des mécanismes tribologiques aux interfaces outils-pièces-copeaux en usinage à sec de l'acier C45. Thèse de Doctorat, Ecole Centrale de Lyon; Ecole Nationale d'Ingénieurs de Monastir
7. Ghouini M, Kouadria KM (2019) Modélisation du contact à l'interface outil-copeau: Approche analytique et numérique. Thèse de Doctorat, Université Ibn Khaldoun de Tiaret
8. Fahrussiam F, Praja IA, Darmawan W, Wahyudi I, Nandika D, Usuki H, Koseki S (2016) Wear characteristics of multilayer-coated cutting tools in milling wood and wood-based composites. Tribol Ind 38:66
9. Labidi C, Collet R, Nouveau C, Beer P, Nicosia S, Djouadi MA (2005) Surface treatments of tools used in industrial wood machining. Surf Coat Technol 200:118–122. https://doi.org/10.1016/j.surfcoat.2005.02.098
10. da Silva LR, da Silva OS, dos Santos FV, Duarte FJ, Veloso GV (2019) Wear mechanisms of cutting tools in high-speed turning of Ti6Al4V alloy. Int J Adv Manuf Technol 103:37–48

Mbakop Nanshie *et al. Journal of Wood Science*   (2024) 70:20

Page 15 of 15

11. Brink T, Molinari J-F (2019) Adhesive wear mechanisms in the presence of weak interfaces: Insights from an amorphous model system. Phys Rev Mater 3:053604
12. Akhtar W, Sun J, Sun P, Chen W, Saleem Z (2014) Tool wear mechanisms in the machining of Nickel based super-alloys: a review. Front Mech Eng 9:106–119
13. Jamil M, He N, Gupta MK, Zhao W, Khan AM (2022) Tool wear mechanisms and its influence on machining tribology of face milled titanium alloy under sustainable hybrid lubri-cooling. Tribol Int 170:107497
14. Straffelini G, Straffelini G (2015) Wear mechanisms. Frict Wear Methodol Des Control 85–113
15. Heidari M (2019) Improvement of cutting tool life for the primary transformation of wood. Dissertation, Université Laval
16. Wei S, Xu L (2019) Review on research progress of steel and iron wear-resistant materials. Acta Met Sin 56:523–538
17. Mazáň A, Vančo M, Barcík Š (2017) Influence of technological parameters on tool durability during machining of juvenile wood. BioResources 12:2367–2378
18. Thibaut B, Denaud L, Collet R, Marchal R, Beauchêne J, Mothe F, Méausoone P-J, Martin P, Larricq P, Eyma F (2016) Wood machining with a focus on French research in the last 50 years. Ann For Sci 73:163–184
19. Ghosh SC, Heidari M, Hernández RE, Blais C (2015) Patterns of knife edge recession in an industrial chipper-canter. For Prod J 65:358–364
20. Nasir V, Cool J (2020) A review on wood machining: characterization, optimization, and monitoring of the sawing process. Wood Mater Sci Eng 15:1–16
21. Bagga PJ, Makhesana MA, Patel KM (2021) A novel approach of combined edge detection and segmentation for tool wear measurement in machining. Prod Eng 15:519–533
22. Jeon S, Stepanick CK, Zolfaghari AA, Lee C (2017) Knife-edge interferometry for cutting tool wear monitoring. Precis Eng 50:354–360
23. Lee J-H, Myagmar G, Kwon H-B, Han J-S (2022) A digital method for wear volume loss analysis using a single-scan three-dimensional dataset. J Dent Sci 17:638–641
24. Platit (2023) Advanced coating systems, Compendium 64. User's manual
25. ASTM G65-04 (2004) Standard test method for measuring abrasion using the dry sand/rubber wheel apparatus. ASTM International, West Conshohocken
26. Wide-Area 3D Measurement System VR-5000/VR-5200. User's manual
27. Tools T-LT with S-PT (1993) International standards, ISO 3685–1993 (E)
28. Mesquita RA (2016) Tool steels: properties and performance. CRC Press, Boca Raton. https://doi.org/10.1201/9781315181516
29. Buchely MF, Gutierrez JC, León LM, Toro A (2005) The effect of microstructure on abrasive wear of hardfacing alloys. Wear 259:52–61. https://doi.org/10.1016/j.wear.2005.03.002
30. Testing AICE-28 on M (2019) Standard test methods for Rockwell hardness of metallic materials. ASTM international, West Conshohocken
31. Krella A (2020) Resistance of PVD coatings to erosive and wear processes: a review. Coatings 10:921
32. Nadolny K, Kapłonek W, Sutowska M, Sutowski P, Myśliński P, Gilewicz A (2020) Experimental studies on durability of PVD-based CrCN/CrN-coated cutting blade of planer knives used in the pine wood planing process. Materials 13:2398
33. Aramesh M, Montazeri S, Veldhuis SC (2018) A novel treatment for cutting tools for reducing the chipping and improving tool life during machining of Inconel 718. Wear 414:79–88
34. Li Y, Schreiber P, Schneider J, Greiner C (2023) Tribological mechanisms of slurry abrasive wear. Friction 11:1079–1093
35. Canale LCF, Albano L, Totten GE, Meekisho L (2014) Hardenability of steel. In: Comprehensive materials processing. Elsevier, pp 39–97. https://doi.org/10.1016/B978-0-08-096532-1.01219-X
36. Xue H, Peng W, Yu L, Ge R, Liu D, Zhang W, Wang Y (2020) Effect of hardenability on microstructure and property of low alloy abrasion-resistant steel. Mater Sci Eng A 793:139901
37. Brajčinović S, Begić Hadžipašić A, Medved J (2022) Inhibitory effect of commercial inhibitor VCI 379/611 on the corrosion behaviour of HTCS-130 tool steel for hot work. Metals 12:966. https://doi.org/10.3390/met12060966
38. Zeisig J, Shtefan V, Giebeler L, Kühn U, Gebert A, Hufenbach JK (2023) A newly designed high-strength tool steel with high wear and corrosion resistance. Materials 16:1941
39. Haus L, Wildfeuer M, Grochowski J-E, Grochowski J-E, Wöckel J, Müller M, Köhn F, Schulz W, Wüstefeld C, Rafaja D, Albrecht J (2022) Wear properties of carbon-rich tungsten carbide films. Wear 488:204146
40. Wärner H (2018) High-temperature fatigue behaviour of austenitic stainless steel: influence of ageing on thermomechanical fatigue and creep-fatigue interaction. Dissertation, Linköping University: Linköping, Sweden
41. Bourbonnais R (2003) Econométrie. Dunod, Paris

Publisher's Note